

## Green machining of Ti6Al4V/Polymers composite made by pellets additive manufacturing

BOSSU Julien<sup>1,a\*</sup>, RIVIÈRE-LORPHÈVRE Edouard<sup>1</sup>, SPITAEELS Laurent<sup>1</sup>,  
DUCOBU François<sup>1</sup>, DELAUNOIS Fabienne<sup>1</sup>, MARTIC Grégory<sup>2</sup>,  
DELMOTTE Cathy<sup>2</sup>, JUSTE Enrique<sup>2</sup>, PETIT Fabrice<sup>2</sup>

<sup>1</sup>University of Mons, Faculty of Engineering, Materials Research Institute, Place du Parc 20,  
7000 Mons, Belgium

<sup>2</sup>BCRC : Belgian Ceramic Research Centre, Avenue du Gouverneur Émile Cornez 4, 7000  
Mons, Belgium

<sup>a</sup>julien.bossu@umons.ac.be

**Keywords:** Green Machining, Ti6Al4V, Polymers, Milling, Pellets Additive Manufacturing

**Abstract.** The poor surface finish (arithmetic roughness  $R_a$  around 40  $\mu\text{m}$ ) of additive manufactured parts leads to the development of hybrid machines to increase the quality of the final part in a lower production time. Hybrid machine already exists for DED (Directed Energy Deposition) and SLS (Selective Laser Sintering) but due to the hardness and the abrasiveness of the sintered material, important tool wear or surface defects on the workpiece can be observed. Therefore, reduced cutting parameters and dedicated cutting tool must then be used which increase the cost of machining operation and the time to produce a part. Green machining can limit these problems: the machining step is performed before sintering when the part does not have its final properties. This kind of material has a pseudo-plastic behavior so machining can be performed with high productivity thanks to lower cutting forces and reduced tool wear. An innovative use of the tool-material couple standard AFNOR Norm NF E66-520 (1999) dedicated to metals is proposed to determine the cutting parameters of a composite based on titanium alloys Ti6Al4V and polymers by measuring surface roughness and cutting forces. A tool dedicated to thermoplastic polymers was tested. Cutting forces and surface roughness (arithmetic surface roughness  $R_a$  and total surface roughness  $R_t$ ) were evaluated for each test. Twelve sets of parameters considering the cutting speed  $v_c$ , the axial depth of cut  $a_p$ , the radial depth of cut  $a_e$  and the feed per tooth  $f_z$  as variables were tested. For the range of parameters selected, it is possible to achieve a satisfactory surface finish with low cutting forces ( $R_a$  remains close to 3.2  $\mu\text{m}$  and cutting forces  $< 5$  N) and stable results.

### Introduction

Pellets Additive Manufacturing PAM is an additive technology similar to FDM (Fused Deposition Modeling) process which uses injection molding pellets as raw material. Pellets are composed of a mix between a metal or ceramic powder (app. 90 wt.%) with a binder (polymer's blend and additives) around 10 wt.% [1,2]. The binder added to the feedstock has many functions compared to the pure metal or ceramic [2]:

- Reducing the abrasiveness of the powder,
- Inducing the rheological properties,
- Influencing the shaping temperature,
- Allowing the creation of porosity during the debinding step.

The method to manufacture a part by PAM technology is composed of 4 steps:

1. Powder blending (metal or ceramic solid loading + binder (blend of polymers and additives))

2. Printing (PAM)
3. Debinding (to remove the binder)
4. Sintering (to give the final mechanical properties to the part) [3]

Nevertheless, additive manufacturing as PAM or FDM process has an inherent disadvantage of additive manufacturing called the staircase effect that often creates a surface finish out of tolerance for industry expectations. Moreover, titanium and its alloys are very difficult to machine at the dense state because of its abrasiveness that causes a huge tool abrasive wear and due to its mechanical properties as a relatively high tensile strength, low ductile yield, 50% lower modulus of elasticity (104 GPa) and approximately 80% lower thermal conductivity than that of steel which create diffusion wear that improve the machining operation cost for dense part [4].

The poor surface finish ( $R_a$  corresponding to the average roughness in the area between the roughness profile and its mean line is around 40  $\mu\text{m}$ ) of parts produced by FDM-like processes requiring finishing machining leads to the development of hybrid machines to increase the quality of the final part in a lower production time [5,6,7].

Hybrid machines already exist for DED (Directed Energy Deposition) and SLS (Selective Laser Sintering) but, due to the hardness and the abrasiveness of the sintered material, important tool wear or surface defects on the workpiece can be observed so reduced cutting parameters have to be selected. A dedicated cutting tool must then be used which increases the cost of machining operation and the time to produce a given part [6].

To address this issue, machining in the raw state, also known as the green state, enables the finishing of parts produced through the additive process before sintering, while the binder is still present. This makes the machining process easier compared to machining sintered materials with all their mechanical properties. Machining in the green state results in parts with mechanical properties similar to those of the polymer used, such as polyamide (e.g. PA66) [8-9].

The aim of this study is to find a wide range of stable cutting parameters to obtain a correct surface quality ( $R_a \leq 3.2 \mu\text{m}$ ) based on a previous study [8] carried out on a raw zirconia/polymer composite and the tool-material couple standard AFNOR NF E66-520 (1999) [10] also proving that this method can be used for all filler/polymer composite materials. In the approach to hybrid use, the cutting forces are also recorded in order to determine whether there is a risk of the workpiece detaching from the build plate during the machining step.

## Material

The experiments were performed using green titanium parts produced on a PAM printer Pollen AM Series MC. The feedstock used is made of 90 wt.% of Ti6Al4V powder and 10 wt% of thermoplastic binder (water-soluble but unknown composition). It is commercialized with the reference polyMIM® Ti6Al4V F 130E (80354) by the PolyMIM GmbH company (Bad Sobernheim, Germany). The geometry of the parts and their main dimensions are given in Fig. 1. It is composed of a cube (20×20 mm) on top of a cylinder (d=15 mm). The cube is first printed (on the building plate) followed by the cylinder. This allows us to obtain the parts without the need for a support structure. The main printing parameters are given in Table 1.

Table 1 : Main printing parameter

Nozzle diameter	1 [mm]
Layer thickness	0.35 [mm]
First layer thickness	0.3 [mm]
Extrusion temperature	250 [°C]
Build platform temperature	70 [°C]
Infill strategy	Lines
Infill percentage	100 [%]
Printing time	28 [min]

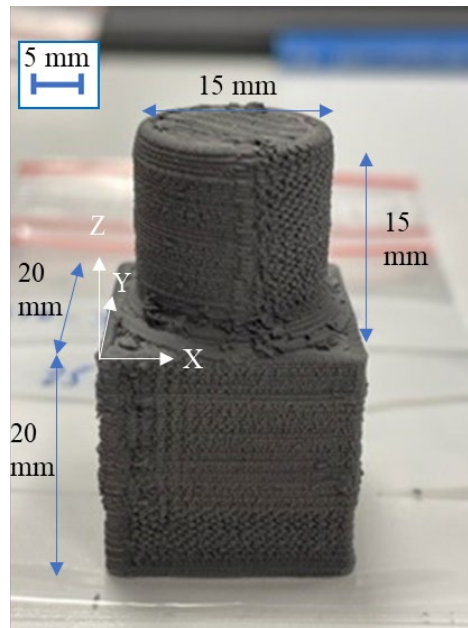


Figure 1 : Part geometry and main dimensions.

### Method

A robotic machining cell composed of a Stäubli TX200 robot fitted with a Teknomotor ATC71 electrospindle was used for the milling operations. The spindle can deliver up to 7.8 kW with a maximal rotational speed of 24000 rpm. A three-jaw chuck was used to clamp the part from the cylinder (Fig. 3) which was attached to a Kistler 9256C2 dynamometer.

The used cutting tool showed in Fig. 2 is originally dedicated to the milling of thermoplastics as PA66. The supplier company is Hoffmann and it's sold with the reference 209425-6. It has a 6 mm diameter with three cutting edges having a double helix angle and a maximal cutting length of 19 mm. It is made in tungsten carbide without any coating.

As presented in a previous study [8], this tool showed great capability to generate smooth and shiny surfaces with  $R_a < 1.6 \mu\text{m}$  in finishing operations [8-9] for composite ceramic/polymer. This study was based on the tool-material couple standard AFNOR NF E66-520-6 (1999) [10] as the present study. Four cutting parameters were used: the cutting speed ( $v_c$ ) corresponding to the speed at which the cutting tool or the workpiece moves relative to each other during machining, the feed per tooth ( $f_z$ ) corresponding to the distance a cutting tool advances per tooth for each revolution of the spindle, the axial depth of cut ( $a_p$ ) representing the depth of the tool's penetration into the workpiece material during a cutting operation, and the radial depth of cut ( $a_e$ ) representing the lateral width of the material removed by the cutting tool. The standard proposes to perform six different experiments [10]: the selection of a stable operating point, the determination of  $v_{c,min}$ , the

determination of minimal and maximal chip thickness ( $h_{min} - h_{max}$ ), the determination of limiting data, the wear tests and the tests to determine the auxiliary parameters. The experiments of the standard allow the determination of the working range for  $v_c, f_z, a_p,$  and  $a_e$  but its full method cannot be applied since the material milled (green metal) as well as the cutting conditions (finishing) are not covered by the standard.

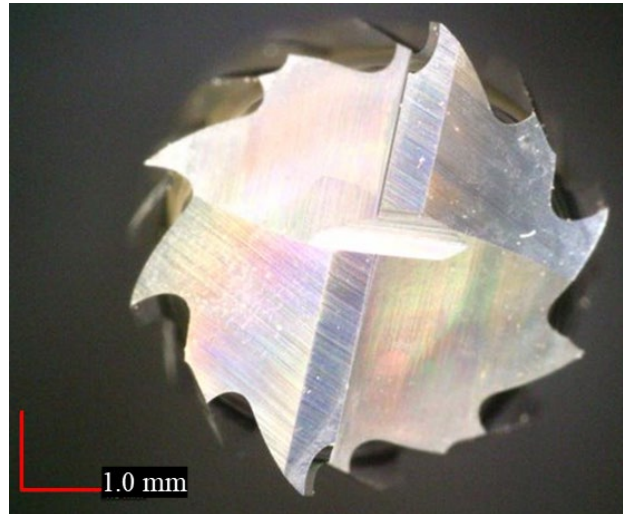


Figure 2 : Microscope image of the milling tool selected for the study.

The initial cutting conditions were selected according to the previous study and are given in Table 2. No lubrication was used for the tests, while compressed air was used between each test to blow the part, the tool and evacuate the chips.



Figure 3 : View of the building part.

A Kistler 9256C2 force sensor was used to record the cutting forces for each pass at a 40 kHz sampling frequency without any filters. The total cutting force (Eq. 1) was considered as a representative value to compare each set of cutting parameters.

The total resulting force (in N) was computed as follows in Eq. 1:

$$F_{tot} = \sqrt{(F_x^2 + F_y^2 + F_z^2)} \tag{1}$$

The first step consists in realizing 3 passes (with radial and axial depths of cut according to Table 2) from the top of the cube (Fig. 1) along the X-axis of the parts.

The arithmetic roughness and the total roughness are then measured, and a microscope view is realized after each pass.

After each step, the generated vertical surface was quantitatively and qualitatively assessed. The cutting forces were recorded for each of the passes. The surface topography was evaluated quantitatively using a Diavite DH6 contact rugosimeter with parameters following the ISO 4288 standard. The arithmetic roughness  $R_a$  was obtained with an evaluation length of 4.8 mm and a cut-off length of 0.8 mm. For all measurements, the probe was displaced according to the parts X-axis (feed direction of the cutting tool). Each vertical surface was characterized by three  $R_a$  and  $R_t$  (corresponding to the vertical distance between the highest and lowest peak within the measured length of a surface profile) measurements, one at the beginning, middle and end of each pass. In total, 36 measurements of roughness were made. The initial surface roughness of the as-built part was estimated using a rugosimeter ZEISS Surfcom 1400. The general aspect of the generated surfaces (porosities, material pull-out) was observed qualitatively using a digital microscope AM7013MZT and the DinoCapture software from DinoLite.

The measurement of the  $R_a$  and  $R_t$  parameters is carried out in order to know what the minimum amount of material to remove in  $a_e$  and to determine if it is possible to be below a  $R_a$  of 3.2  $\mu\text{m}$  which represents the class of mechanical assembly parts, which is very interesting from an industrial point of view.

Table 2 : Set of cutting parameters used during the study.

Configuration	$v_c$ [m/min]	$f_z$ [mm/tooth]	$a_p$ [mm]	$a_e$ [mm]
1	188.4	0.03	3	0.5
2	235.5	0.03	3	0.5
3	282.6	0.03	3	0.5
4	329.7	0.03	3	0.5
5	383	0.03	3	0.5
6	423.9	0.03	3	0.5
7	383	0.026	3	0.5
8	383	0.035	3	0.5
9	383	0.03	3	0.43
10	383	0.03	3	0.58
11	383	0.03	2.6	0.5
12	383	0.03	3.5	0.5

A first set of parameters was tried with  $v_c=383$  m/min based on [8] then a variation of 15% was applied to know if it is a stable point as in the previous study or not. The same was did on  $f_z$ ,  $a_p$  and  $a_e$  to evaluate their impact on the surface roughness and in cutting forces.

### Results

Fig. 4 gives the view of the zones before and after the machining operation of the as-built part. The surface before cutting (blue line) can be seen on the bottom and the surface after cutting (red line) on the top.

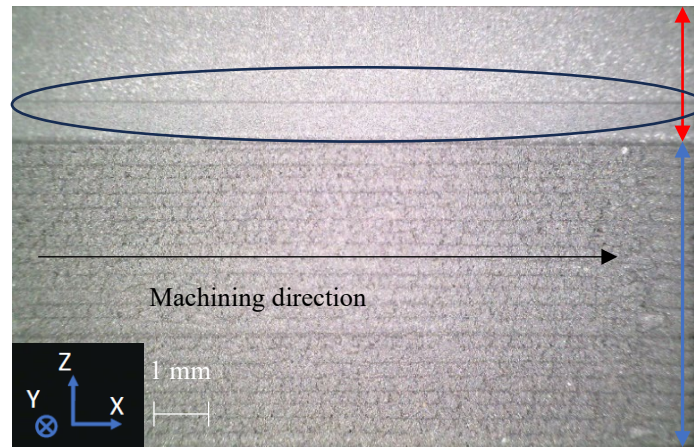


Figure 4: Microscope view of the zone after cutting operations.

The as-built surface topography is very rough on its sides with a  $R_a > 38 \mu\text{m}$ ,  $R_t > 50 \mu\text{m}$  and the zone after machining exhibits a smooth surface. The line presents in this zone machined (surrounded) is due to the geometry of the cutting tool, this line of non-cut material is removed when we go down in the part.

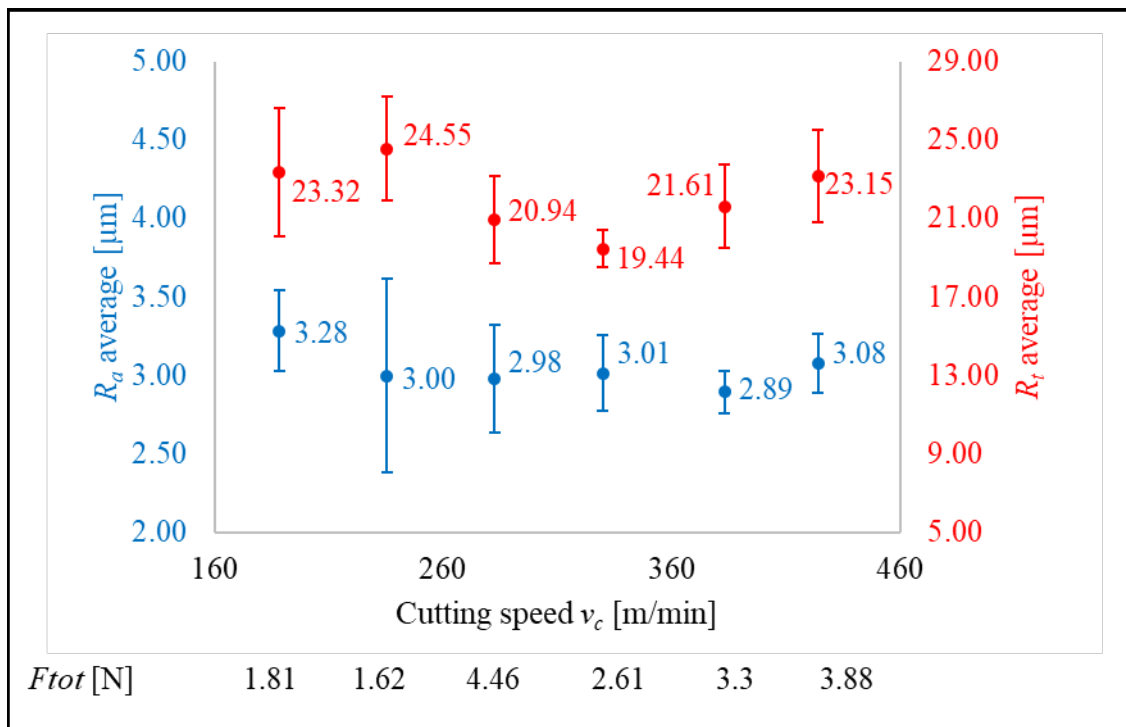


Figure 5: Arithmetic surface roughness  $R_a$  ( $\mu\text{m}$ ), total surface roughness  $R_t$  ( $\mu\text{m}$ ) and cutting forces of the building part after cutting tests depending on the cutting speed  $v_c$  (m/min) corresponding to tests n°1, 2, 3, 4, 5 and 6 (cf. table n°2).

Influence of the cutting speed: Fig. 5 shows the arithmetic and total surface roughness of the machined zone after each test from test n°1 to test n°6 with a constant variation of the cutting speed ranging from 188.4 m/min to 423.9 m/min. The tool showed a great capability to generate a good surface roughness ( $< 3.6 \mu\text{m}$ ). The as-built part has a surface topography with an average  $R_a$  estimated to be between  $2.89 \mu\text{m}$  and  $3.28 \mu\text{m}$  corresponding to a difference of 13.5% and the total roughness  $R_t$  ranges vary from  $19.44 \mu\text{m}$  to  $24.55 \mu\text{m}$  corresponding to a difference of 26%. The best cutting speed range seems to be between 282.6 and 383 m/min with a  $R_a$  difference around

4% and a difference of  $R_t$  around 11%. The cutting forces are low with a minimum of 1.62 N and a maximum of 4.46 N. The cutting forces are  $< 5$  N for each test and there is no material pull out.

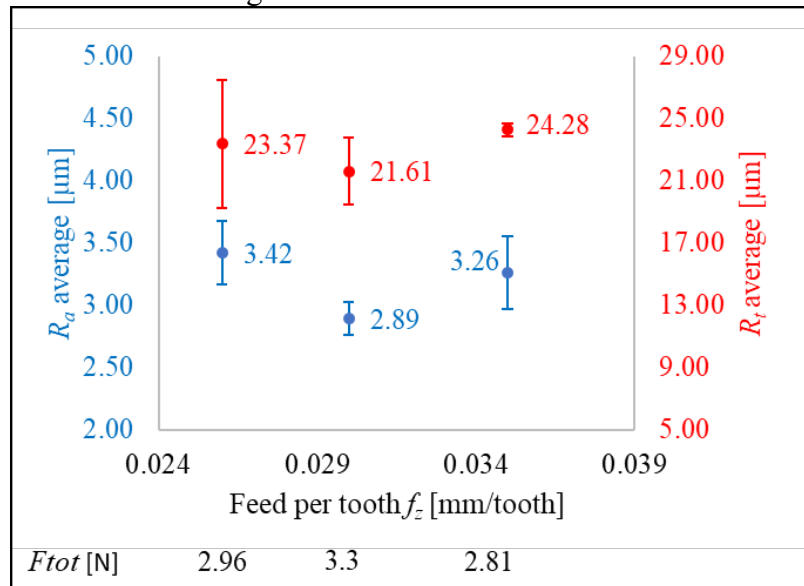


Figure 6 : Arithmetic surface roughness  $R_a$  ( $\mu\text{m}$ ) and total surface roughness  $R_t$  ( $\mu\text{m}$ ) of the building part after cutting tests depending on the feed per tooth  $f_z$  (mm/tooth) corresponding to tests n°5, 7 and 8 (cf. table n°2).

Influence of the feed per tooth: the surface roughness of the part is affected by the feed per tooth in the case of the PolyMIM Ti6Al4V as shown in Fig. 6. In fact, the results exhibit a minimum corresponding to the better and more reproducible  $R_a$  and  $R_t$  measurements for the test n°5 with a feed per tooth of 0.03 mm/tooth (variation of 18% for  $R_a$  and 12% for  $R_t$ ). The variability of the results is evolving for  $R_t$ , more the feed per tooth increases, more the standard deviation in the results increases, reflecting a decrease in the stability of the results as well as an output of the desired arithmetic surface roughness  $R_a < 3.2 \mu\text{m}$ . The cutting forces are stable and between 2.81 and 3.3 N.

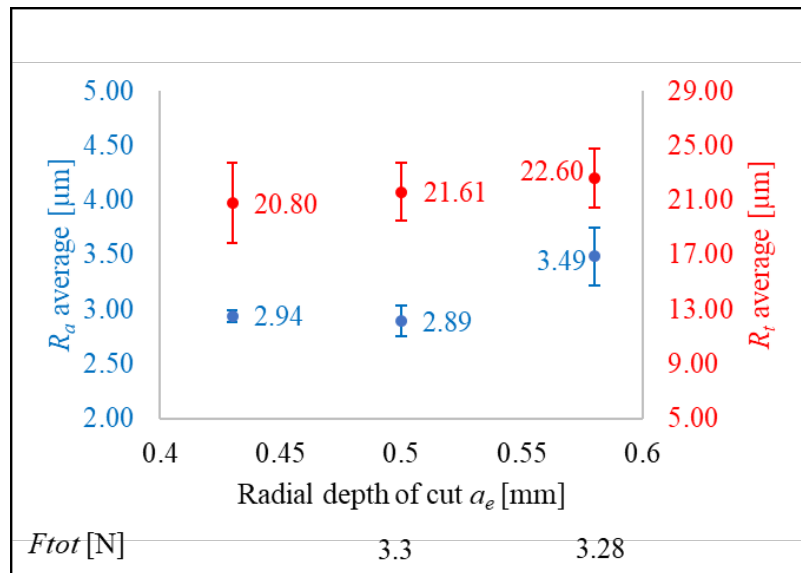


Figure 7 : Arithmetic surface roughness  $R_a$  ( $\mu\text{m}$ ) and total surface roughness  $R_t$  ( $\mu\text{m}$ ) of the building part after cutting tests depending on the radial depth of cut  $a_e$  (mm) corresponding to tests n°5, 9 and 10 (cf. table n°2).

Influence of the radial depth of cut  $a_e$ : the observations of the Fig. 7 show that the radial depth of cut  $a_e$  have a strong impact on the surface roughness of the part. The arithmetic roughness  $R_a$  and the total roughness  $R_t$  increase (around 20% for  $R_a$  and 9% for  $R_t$ ) when  $a_e$  increases between 0.5 and 0.58 mm. The reproducibility of the results is affected too, in fact, the variation grows up between results for a same test with the increase of  $a_e$ . This result shows that optimal  $a_e$  for the used cutting tool is equal or below 0.5 mm. The cutting forces are stable and remains under 3.28 and 3.3 N.

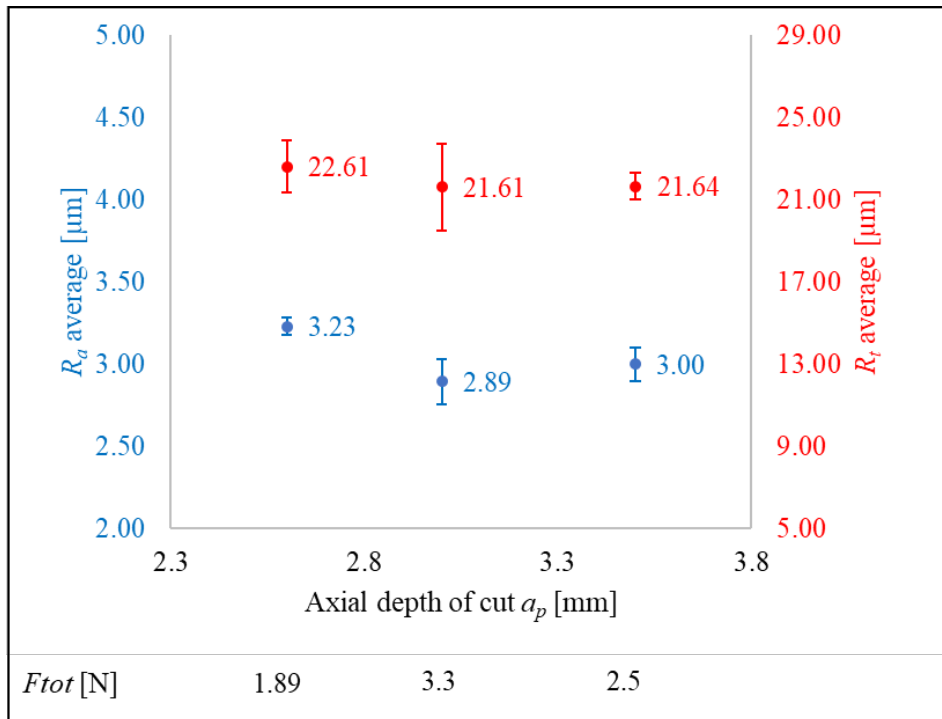


Figure 8 : Arithmetic surface roughness  $R_a$  ( $\mu\text{m}$ ) and total surface roughness  $R_t$  ( $\mu\text{m}$ ) of the building part after cutting tests depending on the axial depth of cut  $a_p$  (mm) corresponding to tests n°5, 11 and 12 (cf. table n°2).

Influence of the axial depth of cut  $a_p$ : the variation of the axial depth of cut  $a_p$  seems to have a slight impact on the surface roughness of the part as shown in Fig. 8. In fact, a maximal variation around 12% for  $R_a$  and 5% for  $R_t$  is present between the minimum and maximum points. All configurations are in the same surface roughness class but the best range of  $a_p$  is from 3 mm.

It can be noted that the cutting forces reach a minimum of 1.89 N and a maximum of 3.3 N, which is similar to the other parameters configurations.

The trends given by the  $R_a$  and  $R_t$  results are globally similar and relatively stable for most of the tested parameters. This is of industrial interest thanks to the wide range of use which allows the operator to choose parameters more easily according to the needs inherent to the equipment used. A set of parameters seems to stand out from the other with better results which correspond to a feed per tooth  $f_z$  of 0.03 mm/tooth, a radial depth of cut  $a_e \leq 0.5$  mm and an axial depth of cut  $a_p = 3$  mm. The feed per tooth, the radial depth of cut and the cutting speed are the parameters with the highest impact on surface roughness in the case of additive manufactured Ti6Al4V part.



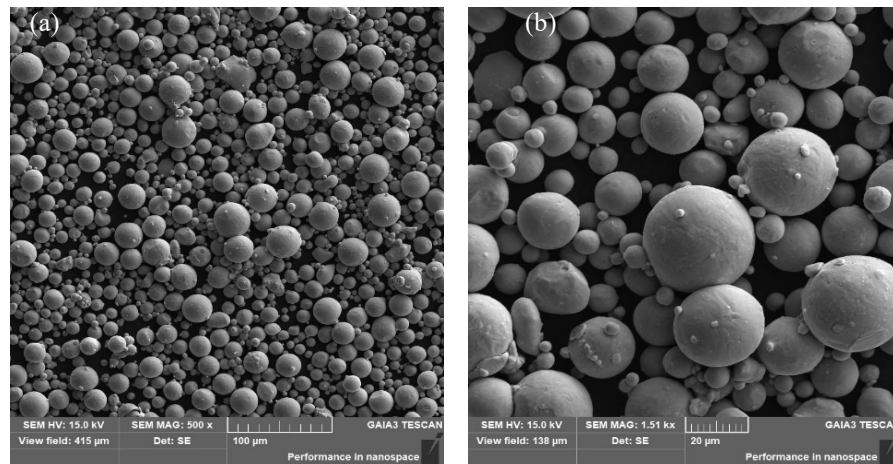


Figure 9 : SEM images of the Ti6Al4V powder of PolyMIM pellets after debinding.

Yoshida [11] did a study to evaluate the impact of grain size and heterogeneity on the surface roughness of sheet metals subjected to plane-strain stretching. According to this work, the surface roughness of parts made by the PolyMIM feedstock does not seem to be able to be significantly improved because of its particle size (average particle size approximatively equal to 20  $\mu\text{m}$ ) and because of the heterogeneity of the particle's sizes according to the SEM images presented on Fig. 9 which represents the particles of PolyMIM Ti6Al4V granule after debinding. The size of the particles is very heterogeneous between approx. 5 and 35  $\mu\text{m}$  and this heterogeneity induces inequality on the surface of the printing and machining part.

The cutting forces were recorded for each cutting test. It's possible to see that all measured values remain under 5 N for each set of cutting parameters. The higher value is for the cutting test n°2 sequence 3 with a value of 4.9 N. The material seems to behave as a polymer more than metal which makes easier the machining operation as confirmed by [8] for ceramic loading.

## Conclusions

This study proves the feasibility of machining composite Ti6Al4V/Polymers parts made by Pellets Additive Manufacturing.

The tool dedicated to thermoplastics polymers seems to be adapted to machine the composite Ti6Al4V / Binder from PolyMIM GmbH.

Total roughness  $R_t$  ranges from 18.49  $\mu\text{m}$  to 28.04  $\mu\text{m}$  and arithmetic roughness  $R_a$  ranges from 2.89  $\mu\text{m}$  to 3.49  $\mu\text{m}$ . The axial depth of cut  $a_p$  has no significant impact on the surface roughness but the feed per tooth  $f_z$ , the radial depth of cut  $a_e$  and the cutting speed  $v_c$  needs to range respectively around 0.03 mm/tooth, inferior or equal to 0.5 mm and between 282.6 and 383 m/min to achieve the objective and not have a change of surface roughness class.

A stable operating point has been find exhibiting a  $R_a < 2.89 \mu\text{m}$  below the objective of 3.2  $\mu\text{m}$  without surface roughness class change and providing an improved generated surface visual appearance.

The cutting forces are below 5 N for each set of cutting parameters which proves that there is no risk of detaching the part from the build plate during machining in the case of a hybrid process.

The proposed approach offers a promising solution for enhancing the quality of additively manufactured titanium parts, reducing post-processing requirements, and potentially optimizing production time. This study makes it possible to quickly obtain qualitatively and quantitatively (visual appearance of the generated machined surface) results since it makes it possible to find machining parameters providing parts with a surface roughness for industrial interest ( $R_a < 3.2 \mu\text{m}$ ) superior to that obtained by additive manufacturing only.

## Perspectives

Further research can follow this one by increase the number of tested set of parameters. Other tools can be used, as tool made especially for the titanium and its alloys or the broader applicability of this method to other materials.

## References

- [1] P. Parenti, S. Cataldo, A. Grigis, M. Covelli, M. Annoni, Implementation of hybrid additive manufacturing based on extrusion of feedstock and milling, *Procedia Manuf.*, Elsevier B.V. 34 (2019) 738–746. <https://doi.org/10.1016/j.promfg.2019.06.230>
- [2] S.C. Altiparmak, V.A. Yardley, Z. Shi, J. Lin, Extrusion-based additive manufacturing technologies: State of the art and future perspectives. *J. Manuf. Process.* 83 (2022) 607–636. <https://doi.org/10.1016/j.jmapro.2022.09.032>
- [3] R. Eickhoff, S. Antusch, D. Nötzel, T. Hanemann, New Partially Water-Soluble Feedstocks for Additive Manufacturing of Ti6Al4V Parts by Material Extrusion. *Materials* 16 (2023). <https://doi.org/10.3390/ma16083162>
- [4] E.O. Ezugwu, Z. Wang, M. Materials Processing Technology Titanium alloys and their machinability a review. *J. Mater. Process. Technol.* 68 (1997) 262-274. [https://doi.org/10.1016/S0924-0136\(96\)00030-1](https://doi.org/10.1016/S0924-0136(96)00030-1)
- [5] B.N. Turner, S.A. Gold, A review of melt extrusion additive manufacturing processes: II. Materials, dimensional accuracy, and surface roughness. *Rapid Prototyp. J.* 21/3 (2015) 250–261. <https://doi.org/10.1108/RPJ-02-2013-0017>
- [6] J.M. Flynn, A. Shokrani, S.T. Newman, V. Dhokia, Hybrid additive and subtractive machine tools – Research and industrial developments. *Int. J. Mach. Tools Manuf.* 101 (2016) 79–101. <http://dx.doi.org/10.1016/j.ijmachtools.2015.11.007>
- [7] A. Demarbaix, M. Mulliez, E. Rivière-Lorphèvre, L. Spitaels, C. Duterte, N. Preux, F. Petit, F. Ducobu, Green Ceramic Machining: Determination of the Recommended Feed Rate for Y-TZP Milling. *J. Compos. Sci.* 5 (2021) 231. <https://doi.org/10.3390/jcs5090231>
- [8] L. Spitaels, H. Dantinne, J. Bossu, E. Rivière-Lorphèvre, F. Ducobu, A Systematic Approach to Determine the Cutting Parameters of AM Green Zirconia in Finish Milling. *J. Compos. Sci.* 7 (2023)112. <https://doi.org/10.3390/jcs7030112>
- [9] L. Spitaels, E. Rivière-Lorphèvre, G. Martic, E. Juste, F. Ducobu, Machining of PAM green Y-TZP: Influence of build and in-plane directions on cutting forces and surface topography. *Materials Research Proceedings* 28 (2023) 1245-12. <https://doi.org/10.21741/9781644902479-135>
- [10] NF E66-520-6; Working Zones of Cutting Tools. Couple Tool–Material. Association Française de Normalisation AFNOR : Paris, France, 1999.
- [11] K. Yoshida, Effects of grain-scale heterogeneity on surface roughness and sheet metal necking. *Int. J. Mech. Sci.* 83 (2014) 48–56. <https://doi.org/10.1016/j.ijmecsci.2014.03.018>